Journal of Applied Physics

Intrinsic surface passivation of CdTe

Cite as: J. Appl. Phys. **118**, 155305 (2015); https://doi.org/10.1063/1.4933186
Submitted: 06 July 2015 . Accepted: 23 September 2015 . Published Online: 21 October 2015

M. O. Reese, C. L. Perkins, J. M. Burst, S. Farrell, T. M. Barnes, S. W. Johnston, D. Kuciauskas, T. A. Gessert, and W. K. Metzger

JOURNAL OF APPLIED PHYSICS **118**, 155305 (2015)

Intrinsic surface passivation of CdTe

M. O. Reese, C. L. Perkins, J. M. Burst, S. Farrell, T. M. Barnes, S. W. Johnston, D. Kuciauskas, T. A. Gessert, and W. K. Metzger
National Renewable Energy Laboratory, Golden, CO 80401, USA

(Received 6 July 2015; accepted 23 September 2015; published online 21 October 2015)

Recombination is critically limiting in CdTe devices such as solar cells and detectors, with much of it occurring at or near the surface. In this work, we explore different routes to passivate p-type CdTe surfaces without any intentional extrinsic passivation layers. To provide deeper insight into the passivation routes, we uniquely correlate a set of characterization methods: surface analysis and time-resolved spectroscopy. We study two model systems: nominally undoped single crystals and large-grain polycrystalline films. We examine several strategies to reduce surface recombination velocity. First, we study the effects of removing surface contaminants while maintaining a near-stoichiometric surface. Then we examine stoichiometric thermally reconstructed surfaces. We also investigate the effects of shifting the surface stoichiometry by both "subtractive" (wet chemical etches) and "additive" (ampoule anneals and epitaxial growth) means. We consistently find for a variety of methods that a highly ordered stoichiometric to Cd-rich surface shows a significant reduction in surface recombination, whereas a Te-rich surface has high recombination and propose a mechanism to explain this. While as-received single crystals and as-deposited polycrystalline films have surface recombination velocities in the range of 10^5–10^6 cm/s, we find that several routes can reduce surface recombination velocities to $<2.5 \times 10^4$ cm/s. © *2015 AIP Publishing LLC*.
[http://dx.doi.org/10.1063/1.4933186]

INTRODUCTION

Charge carrier recombination limits device performance in CdTe devices such as solar cells and radiation detectors. Much of this recombination occurs at or near the surface. Typically, the surface recombination velocity (SRV) is in the range of 10^5–10^7 cm/s for CdTe polycrystalline films or high quality single crystals.[1–4] This is comparable to *bare* GaAs,[5,6] but it is unacceptably high for devices particularly when compared to passivated GaAs or Si. For instance, even low resistivity p-type Si has typical SRV values of 50–500 cm/s when passivated with a thermal oxide; 20–50 cm/s when using the "Alneal process" (which utilizes an additional Al evaporation and anneal to reduce the Si-SiO_2 interfacial density); and <1–10 cm/s with other surface preparation techniques and/or doping.[7–9] Advances in surface passivation led to the first c-Si solar cells that exceeded 20% one-sun efficiencies in the 1980s;[10] similar advances enabled GaAs-based solar cells to exceed 24% efficiencies.[11,12]

CdTe photovoltaic devices have been commercialized with remarkable success,[13] with costs per watt that are competitive with silicon modules, despite lower efficiencies.[14] For years, the record efficiencies of CdTe research cells had stagnated between 16% and 17%.[15,16] Recently, there have been dramatic improvements in CdTe device efficiencies, and the present record is 21.5%.[17–20] Most of these gains (~2.5% absolute) have been due to increased photocurrent density, with an advance from 26.1 mA/cm^2 to 30.25 mA/cm^2.[16,20] An ~1% absolute gain has resulted from an increase in fill factor.[16,20] The open-circuit voltage in record devices has remained low, in the range of 845–875 mV, despite the 1.45 eV bandgap of CdTe.[17–20] Future efficiency gains now require overcoming this voltage barrier. The low doping (10^{13}–10^{15} cm^{-3}) and low minority carrier lifetimes typically observed in polycrystalline material have been identified as the most significant limitation of open-circuit voltage.[21,22] For short bulk minority carrier lifetimes (i.e., <10 ns) and low doping, there is a roughly equal tradeoff for open-circuit voltage. Once lifetimes exceed ~10 ns, increasing doping becomes critical.[21,23] There is strong experimental correlation between open-circuit voltage and the near-surface minority carrier lifetime.[3] Here, we investigate methods to increase the near-surface lifetime in order to increase open-circuit voltage.

CdTe photovoltaic devices have evolved very differently than Si and GaAs. Si and GaAs photovoltaic devices have benefitted from the concurrent growth of the integrated circuit and laser industries. These combined markets have led to the availability of high quality single-crystal materials as well as extensive bodies of literature on their properties. In contrast, the evolution of CdTe technology has been primarily driven by small improvements in polycrystalline film properties and device fabrication. CdTe for photovoltaics is typically deposited extremely quickly and followed by a complex series of post-treatments and anneals to improve the material. Instead of controlled *in-situ* doping, p-type polycrystalline CdTe is usually fabricated with a combination of intrinsic defects and impurity diffusion during and after growth. Standard growth processes yield a Te-rich defect chemistry.[24] After CdTe deposition, films are annealed in $CdCl_2$ and O_2, and generally annealed again after the deposition of a Cu-containing back contact on a surface prepared with a Te-rich stoichiometry.[25–30] These steps lead to thermal diffusion of S, O, Cl, and Cu into the CdTe layer,[31] which has been observed to increase passivation, near-surface minority carrier lifetimes,

and/or open circuit voltage.[32–35] Cl and Cu appear to have the most dramatic effects, enabling the lifetimes and efficiencies observed in state-of-the-art PV devices.[3,4] However, it is likely that this convoluted defect chemistry is at least partly responsible for the stagnant open-circuit voltage and high recombination observed in CdTe solar cells.

Recently, we have revisited some basic assumptions about the fundamental material properties of CdTe.[31,36] An earlier theoretical model using a local density approximation (LDA) suggested that the Te vacancy (V_{Te}) could be the most detrimental deep-level defect in intrinsic CdTe.[37] Due to the fact that the LDA model underestimates the bandgap, its defect level predictions were reexamined with the Heyd-Scuseria-Ernzerhof 2006 (HSE06) hybrid functional theoretical model.[36] This new theoretical framework predicts a Cd-rich defect chemistry will have fewer deep defects with low formation energy than a Te-rich defect chemistry.[31,36] In this model, the V_{Te} becomes a shallow donor, Te antisites (Te_{Cd}) and Te interstitials (Te_i) become the dominant mid-gap deep levels, and the Cd vacancy (V_{Cd}) becomes a deeper acceptor ($\sim$0.36 eV above the valence band maximum).[31] This theoretical framework was then supported with experimentally grown off-stoichiometric samples that exhibited higher *bulk* recombination in Te-rich samples than Cd-rich ones (near-surface recombination remained the same).[36]

Experimental results have shown that exposing the back surface of a CdTe PV device to Te was correlated with a drop in minority-carrier lifetime and device performance.[38] This result was surprising because high efficiency back contacts have historically required a thick Te-rich layer prior to making the back contact for CdTe PV devices (typically with a wet etch such as Br_2:MeOH or nitric-phosphoric acid). The formation of this layer generally precedes a Cu-diffusion step that serves the role of both doping the CdTe as well as reducing the back contact barrier height through the formation of a thin Cu_xTe or Te layer.[39,40]

Here, we explore how the SRV correlates with shifts in the intrinsic surface defect chemistry. Surface recombination/passivation studies in CdTe have been limited and most previous reports on this topic have, in general, focused on improving the SRV (or near-surface minority carrier lifetime) in CdTe and CdTe alloys (e.g., HgCdTe and CdZnTe)[2,34,41] using extrinsic dopants and passivants including S, O, Cl, Zn, and In[2,4,32,34,35,42,43] to achieve surface recombination velocities as low as 200–2000 cm/s in doped n-type CdTe single crystals and p-type $Hg_{1-x}Cd_xTe$ crystals.[2,42] Reports of passivation of *p-type* CdTe are limited to SRVs of 6–40 $\times 10^4$ cm/s, without the use of double heterostructures.[32,44] Furthermore, the best results were unstable to air exposure and the more modest values use S as a passivant.

In this work, we study p-type CdTe single crystals and large-grain polycrystalline films on bare glass as experimental "model" systems with *no* intentional extrinsic defects such as S, O, Cl, or Cu. We believe an alternate defect chemistry (e.g., no copper impurities) will ultimately be necessary to significantly improve the open-circuit voltage, so here we explore the limits of *intrinsic* CdTe surface passivation.

We use a detailed approach in which we use *in situ* surface analysis techniques and correlate them with time-resolved spectroscopy measurements. Using this characterization approach provides new insight into the surface passivation/recombination. This has not been in the past done with CdTe; a similar correlated approach is infrequently seen for other semiconductor systems. Here, we first focus on the effects of removing surface contaminants while maintaining a near-stoichiometric surface. Second, we study stoichiometric, thermally reconstructed surfaces. Last, we examine the effects of shifting the surface stoichiometry to both Te-rich and Cd-rich conditions by both "subtractive" and "additive" means. The "subtractive" method alters the surface stoichiometry with wet chemical etches. We also use two different "additive" methods: (1) ampoule anneals with Cd/Te-rich ambients to alter the defect chemistry and (2) epitaxial growth of thin Cd/Te layers. Through this examination of a large variety of methods, we show that a highly ordered stoichiometric or Cd-rich surface has a significant benefit relative to a Te-rich surface. Last, we propose a mechanism that is consistent with these results.

EXPERIMENTAL METHODS

Sample preparation

Our two "model" systems were p-type (10^{14} cm^{-3}) intrinsic CdTe single crystals (100) from JX Nippon Mining & Metals and large-grain polycrystalline films grown on glass (Corning 7059) by close-space sublimation (CSS). The single crystals were measured as-received as well as with a variety of treatments described below. The large-grain polycrystalline films were deposited via CSS in a system with a base pressure ca. 10^{-2} Torr, then backfilled to a pressure of 20 Torr with UHP hydrogen. Films were grown with a source temperature of 700 °C and a substrate temperature of 600 °C over the course of 60–75 min., generating films >100 μm thick with typical grain sizes in the range of 20–100 μm. These films were then used as-deposited as well as with a variety of treatments as described below.

Samples prepared by ampoule annealing used as-received single crystals sealed in ampoules evacuated to 10^{-5} Torr with 7 N shot of either Cd or Te. The samples were later annealed in a tube furnace at 700 °C for 2 h. After an anneal was completed, the ampoule was removed from the furnace and quenched in water.

Samples prepared by molecular beam epitaxy (MBE) used single crystals. Prior to loading in the MBE chamber, each wafer was etched in a 0.5% bromine:methanol solution for 10 s (etching at $\sim$0.75 μm/min), rinsed in methanol, dried, then quickly loaded into the system using indium-free substrate holders. Upon transfer into the growth chamber, the surfaces have a thin Te-rich layer as observed by reflected high energy electron diffraction (RHEED). *In situ* deoxidization was performed at a temperature of $\sim$300 °C for 5 min under a Te or Cd overpressure to ensure that the surface remained smooth. The samples were allowed to cool to $\sim$250 °C before the overpressure was shuttered. The samples were then allowed to cool to $\sim$150 °C and <100 °C for Te and Cd capping layers, respectively. The Te and Cd

capping layers were deposited onto the samples for 15, 35, and 75 s. Te was deposited at an estimated rate of 2.5 Å/s. For 35 s, this corresponds to a thickness of ~8.7 nm. RHEED analysis shows evidence of an amorphous Te layer for each of these samples. Cd was deposited at an estimated rate of 1.3 Å/s. An amorphous Cd layer was only observed at the end of the 75 s Cd deposition.

A series of nine wet etchants were prepared in the following manner.

(1) 10 ml of nitric acid (HNO_3) were mixed with 4 g of potassium dichromate ($K_2Cr_2O_7$) in 20 ml of distilled water.
(2) 10 ml of nitric acid (HNO_3) were mixed with 4 g of potassium dichromate ($K_2Cr_2O_7$) and 5 g of copper nitrate ($CuNO_3$) in 20 ml of distilled water and 0.25 ml of hydrofluoric acid (HF).
(3) A 2.5 M solution of ferric chloride ($FeCl_3$) solution was prepared with water.
(4) 2.2 ml of nitric acid (HNO_3) were mixed with 175 ml of phosphoric acid (H_3PO_4) and 170 ml of distilled water.
(5) 2 ml of acetic acid (CH_3COOH) were mixed with 10 ml of nitric acid (HNO_3) and 3.2 ml of sulfuric acid (H_2sO_4).
(6) 0.8 g of sodium hydroxide (NaOH) and 1.05 g of $Na_2S_2O_4$:H_2O were dissolved in 70 ml of distilled water.
(7) For a potassium hydroxide etch, a Transene PSE200 solution with a ratio of 1:7 KOH:H_2O was used.
(8) 0.5%, 1%, and 2% bromine in methanol (Br_2:MeOH) were prepared by adding 50, 100, or 200 μl to 10 ml of MeOH. These were prepared fresh and used within minutes of preparation.
(9) A 2 M hydrazine (N_2H_4) solution was prepared in methanol and kept in a nitrogen filled glovebox.

Solutions 1–8 were used in a 30 s, room temperature etch for initial characterization. The KOH etch (7) was utilized over a wider range of conditions, with varying time and temperature. It was found to be quite sensitive to these variables with a 15 s etch at 50 °C yielding similar near-surface lifetimes to a 300 s etch at 40 °C. The 1% Br_2:MeOH solution was used in 60 s etches by itself (removing ~2.5 μm/min) as well as prior to a 15 min 2M hydrazine (N_2H_4) soak in a nitrogen filled glovebox. The 2% Br_2:MeOH etch was performed for 5 min (removing ~5.5 μm/min) prior to a 3 min KOH etch, sputter cleaning, and/or thermal anneals to remove polishing damage. Wet etches were performed in both air and a nitrogen filled glovebox with no discernible difference in near-surface lifetimes, except for the N_2H_4 soak. Glovebox thermal anneals were performed on a hotplate, with sequential 10 min anneals at 225 °C, 275 °C, and 325 °C as measured with a surface thermometer. Time-resolved photoluminescence (TRPL) measurements were performed between anneals to find optimum conditions.

Characterization techniques

Time resolved optical spectroscopy was applied to accurately determine minority carrier lifetimes and surface recombination velocities. This analysis is based on different carrier generation spatial profiles with one-photon and two-photon excitation (1PE and 2PE, respectively). When 2PE with low energy (sub-bandgap, 1120 nm) photons is focused >100 μm from the surface of the sample, bulk properties (τ_{bulk}) could be accurately evaluated.[45–47] (The estimated 2PE excitation volume is ~6 μm wide by ~20 μm deep; typical carrier diffusion length <20 μm.) Because of the large absorption coefficient of CdTe ($\alpha_{650\,nm} = 46\,000\,cm^{-1}$),[48] the excitation at 650 nm had an absorption depth of ~220 nm. Time resolution of experimental measurements was ~20 ps, therefore, carrier decay rates from the generation location could be accurately resolved by using time-correlated single photon counting. Therefore, spatial resolution of reported optical analyses is <200 nm, and this data accurately reflect near-surface properties. Two groups have developed models for estimating surface recombination velocities (SRV) from time-resolved spectroscopy data. Wang *et al.*[45] have shown that initial decay rate $1/\tau_1$ is

$$\frac{1}{\tau_{av}} = \frac{1}{\tau_B} + \frac{2\alpha^2 D}{1+\sqrt{1+8\alpha^2 D^2/S^2}} \approx \frac{1}{\tau_B} + \frac{\alpha}{\sqrt{2}}S, \quad (1)$$

where Ahrenkiel and Dashdor have derived[49]

$$\frac{1}{\tau_1} = \frac{1}{\tau_B} + \alpha S. \quad (2)$$

The difference for SRV analysis with Eqs. (1) and (2) is sqrt(2), which indicates uncertainty in SRV values derived from simplified optical analysis. To test the validity of Eqs. (1) and (2) for surface recombination analysis in CdTe, we applied detailed TCAD simulations and found good agreement between the results derived from detailed simulations and models of Eqs. (1) and (2).[44]

The laser repetition rate was 2–10 MHz (1PE) and 1.1 MHz (2PE). Time resolved photoluminescence (TRPL) was measured with a 715 nm long-pass filter for 1PE-TRPL and with a 10 nm band-pass filter centered at 840 nm for 2PE-TRPL. The red shift with excitation in the bulk is attributed to reabsorption.[46]

Two exponential data analysis model with deconvolution of the instrumental response (IRF) was used in the data analysis

$$PL = A_1 \exp(t/\tau_1) + A_2 \exp(-t/\tau_2), \quad (3)$$

where A_1/A_2 are amplitudes of the decay components τ_1/τ_2 and t is time. As described above, the initial decay $1/\tau_1$ is taken to indicate near-interface recombination based on the models of Eqs. (1) and (2). For well-passivated surfaces, τ_2 will approach the bulk lifetime measured with a 2PE measurement, however, for poorly passivated surfaces the near-surface recombination dominates the measurement such that τ_2 can be orders of magnitude lower than the true bulk lifetime.

Surface composition was measured by x-ray photoemission spectroscopy (XPS) using the Physical Electronic 5600 portion of a cluster tool that has been described previously.[50] Core-level spectra were obtained using monochromatic Al K_α radiation and analyzed using the Physical Electronics

MultiPak V9.0 software package. Spectra were taken using a pass energy of 11.75 eV at normal takeoff angle. Prior to surface modifications performed in ultrahigh vacuum (UHV), crystals were etched in a 2% Br_2:MeOH solution for 300 s to remove polishing damage. Surface modifications performed in the XPS system were heating, argon ion sputtering, and exposure to atomic hydrogen. Temperatures were measured using a type K thermocouple pressed against the top of samples and a Eurotherm 2204 e controller. During typical UHV annealing cycles to 250 °C, a temperature at which there is minimal sublimation of CdTe, the chamber pressure was less than 5×10^{-8} Torr. Argon ion sputter cleaning used a focused 3 kV beam at 2 μA/cm^2. Atomic hydrogen was produced in a thermal process using an Oxford Applied Research TC-50 cracker at a beam equivalent pressure of 1×10^{-6} Torr. Crystals were held at 90 °C during hydrogen cleaning. Low energy electron diffraction (LEED) measurements were conducted using an Omicron MCP-SPECTALEED system equipped with double microchannel plates.

Hall measurements were performed on representative samples in a van der Pauw configuration with graphite contacts (AquaDAG paste) to determine carrier concentration, mobility, and type using a BioRad HL5500.

RESULTS AND DISCUSSION

Untreated single crystals and large-grain polycrystalline films

The literature reports very poor surface quality of single crystals, even after "final" chemical-mechanical polished surfaces.[1,2] Using 1PE-TRPL and 2PE-TRPL, we examined as-received (100), (111)A, (111)B, (211)A, and (211)B single crystals. A summary of all of the different treatments and fitted parameters from this study, including τ_1, τ_2, and surface recombination velocity, appear in Table I.

Typically, we measure near-surface lifetimes in the range of 4–90 ps for untreated samples. This leads to SRVs in the range of 2.4–50 $\times 10^6$ cm/s for as-received single crystals. We observed no correlation between surface recombination velocity and crystal orientation or A/B termination for as-received single crystals. This is likely because all had oxidized and/or damaged surfaces. Figure 1 indicates that these values are remarkably similar to those observed for as-grown polycrystalline films (3–15 $\times 10^6$ cm/s), even though the samples have different surface-to-bulk ratios. The bulk lifetimes as measured with 2PE-TRPL of these samples were all considerably longer, with the single crystals all in the range of 80–140 ns (Figure 1). In contrast, multiple large-grain

TABLE I. Summary of extracted surface recombination properties for various samples examined in this work.

Substrate	Treatment	Cd:Te Ratio	t_1 (ps)	t_2 (ps)	SRV (cm/s)
SX	Untreated	…	4–90	470–725	2.4–50 $\times 10^5$
[PX]			[15–70]	[210–390]	[3.2–15 $\times 10^5$]
SX	Br_2:MeOH/atomic hydrogen	…	180	1200	1.2 $\times 10^5$
SX	Br_2:MeOH/sputter clean (N_2)	…	60	1400	3.6 $\times 10^5$
SX	Br_2:MeOH/sputter clean (Ar)	1.08–1.09	170	2600	1.3 $\times 10^5$
SX	Br_2:MeOH/sputter clean (Ar)/UHV thermal anneal	1.09	600–850	16000–19000	2.6–3.6 $\times 10^4$
SX	As-received/hotplate anneal	…	130–170	950–970	1.3–1.7 $\times 10^5$
SX	Br_2:MeOH/hotplate anneal	…	580–670	6000–8400	3.2–3.7 $\times 10^4$
SX	Br_2:MeOH/KOH/hotplate anneal	…	830	11700	2.6 $\times 10^4$
SX	Br_2:MeOH/KOH/hotplate anneal/Br:MeOH	…	85	610	2.6 $\times 10^5$
SX	Ampoule anneal with Te-ambient	1.05 (high carbon signal)	140–190	690–1600	1.1–1.6 $\times 10^5$
SX	Ampoule anneal with Cd-ambient	1.28 (high carbon signal)	720–1100	8700–9400	2–3 $\times 10^4$
SX	1% Br_2:MeOH (60 s)	0.73	60	460	3.6 $\times 10^5$
[PX]			[70]	[450]	[3 $\times 10^5$]
[PX]	HNO_3:H_3PO_4	…	[75]	[660]	[3 $\times 10^5$]
SX	$FeCl_3$	0.034	35	410	6.2 $\times 10^5$
[PX]			[15]	[230]	[1.7 $\times 10^6$]
SX	HNO_3:$K_2Cr_2O_7$	0.062	75	700	2.9 $\times 10^5$
[PX]			[65]	[430]	[3.3 $\times 10^5$]
SX	HNO_3:$K_2Cr_2O_7$:$Cu(NO_3)_2$	0.085	70	580	3.1 $\times 10^5$
[PX]			[80]	[380]	[2.7 $\times 10^5$]
SX	CH_3COOH:HNO_3:H_2SO_4	0.0037	30	390	7.2 $\times 10^5$
[PX]			[10]	[155]	[2 $\times 10^6$]
SX	KOH	1.12	240–330	2400–3000	6.6–9.1 $\times 10^4$
[PX]			[590–640]	[4100–5900]	[3.7 $\times 10^4$]
SX	NaOH:$Na_2S_2O_4$	1.35	200	1500	1.1 $\times 10^5$
[PX]			[320–1100]	[5900–9500]	[2–6.8 $\times 10^4$]
SX	Br_2:MeOH/N_2H_4	0.86	300–340	920–3000	6.4–7.2 $\times 10^4$
[PX]			[160]	[760]	[1.3 $\times 10^5$]
SX	Br_2:MeOH/KOH	…	350	3900	6.2 $\times 10^4$
SX	0.5% Br_2:MeOH (10 s)/vacuum thermal reconstruction/MBE Cd (35 s)	…	1150	23700	1.9 $\times 10^4$
SX	0.5% Br_2:MeOH (10 s)/vacuum thermal reconstruction/MBE Te (35 s)	…	40	560	5.4 $\times 10^5$

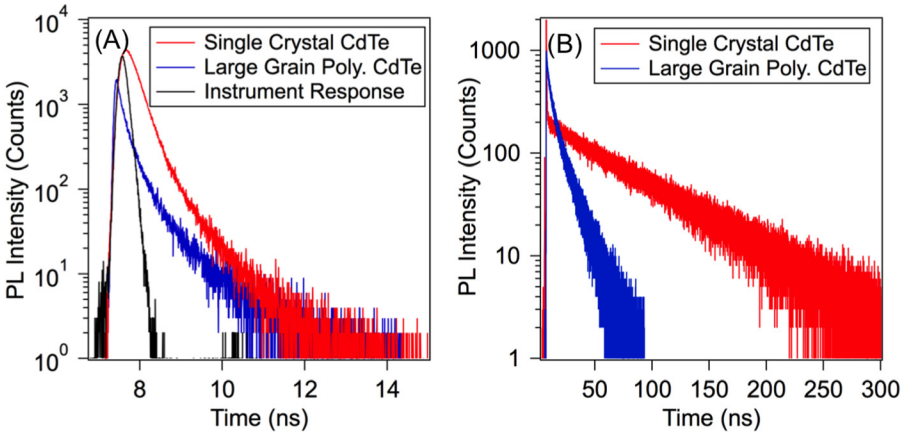

FIG. 1. Representative time-resolved photoluminescence measurements of single-crystal CdTe and large-grain polycrystalline CdTe films on glass. (a) one-photon excitation TRPL measurements, which measures aggregate, near-surface minority-carrier lifetime, (b) two-photon excitation TRPL measurements, which measures bulk minority carrier lifetime.

polycrystalline CdTe films were measured with 2PE-TRPL to have bulk lifetimes of 6–14 ns across individual 1.5 in. square samples (Figure 1). This may be an indication of the sample non-uniformity, variation in grain size, or excitation volumes that include varying amounts of bulk/grain boundaries. As mentioned previously, the surface recombination in these films was very similar to as-deposited small grain (i.e., 1's of μm) polycrystalline films typical of standard PV devices as well as in single crystals. The large difference between the 1PE-TRPL (surface sensitive) and 2PE-TRPL (bulk sensitive) measurements indicates that electronic properties of these samples are completely surface dominated. To simplify the presentation of our results, we will limit discussion to surface recombination velocities, but the interested reader should refer back to Table I.

XPS measurements show that as-received single-crystal samples were heavily oxidized with silicon, chlorine, and carbon contamination present on the surface. Figure 2 shows representative XPS spectra of an as-received crystal and of another that had been cleaned by sputtering and UHV annealing. Silicon contamination may be attributed to one of a few sources. First, the samples were shipped attached to a mild adhesive carrier film, which may be Si-containing (e.g., polydimethylsiloxane) that migrated to the front surface. Second, a quartz crucible may have been used during

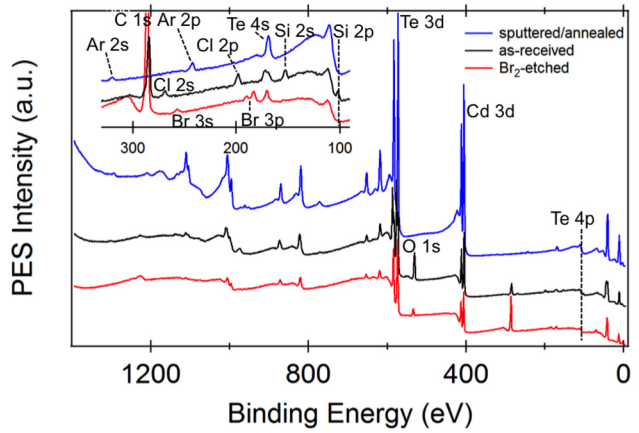

FIG. 2. XPS survey spectrum of sputter-cleaned/annealed, bromine-etched, and as-received CdTe(100) crystal. Inset shows carbon, chlorine, and silicon signals from the as-received crystal, argon peaks on the sputter-cleaned crystal, and residual bromine on the etched crystal.

growth. Third, the samples may have experienced a polishing step with silica-based particles. Scanning electron microscopy paired with energy dispersive x-ray spectroscopy has shown that there can be silica-containing nanoparticles embedded in the sample surface. Deep (e.g., microns) subsurface polishing damage in CdTe can also be revealed by chemical etching. This extensive damage could be expected to lead to high surface recombination velocity in as-received wafers. Studies with optical microscopy/profilometry indicate that the polishing damage can be removed after chemically etching $\sim$7 μm of material.[51] We also observed that samples that had been mechanically polished at NREL exhibited even higher surface recombination and drastic reductions in the photoluminescence intensity.

Effects of removing surface contaminants and deep subsurface damage

Many CdTe surface cleaning procedures in the literature include an etch in Br_2:MeOH. An XPS survey scan (shown in Figure 2) showed that etching a single-crystal wafer in Br_2:MeOH resulted in a surface that had elemental tellurium (i.e., Te^0 instead of just Te^{2-} as part of the CdTe matrix) as well as substantial oxygen, carbon, and bromine. The presence of elemental tellurium is noted from broadening of the Te $3d_{5/2}$ peak width found on the etched crystal results from the superposition of peaks from Te^0 and Te^{2-}; Te^0 is found at 0.70 eV higher binding energy than the Te^{2-} that is part of the CdTe lattice.[52] Argon sputtering of CdTe has been shown to leave a stoichiometric surface, although the process may leave residual surface and subsurface damage. As expected, crystals cleaned by argon sputtering appeared clean and stoichiometric by XPS (Table II). Ar sputter-cleaned samples left a nominal Cd:Te ratio of 1.08–1.09. Atomic hydrogen cleaning has been shown to remove oxides and carbon from surfaces,[53] whereas sputtering should be indiscriminate and could produce electronically active defects. In our setup, atomic hydrogen was effective in removing oxygen, but not carbon (Table II). Figure 3 shows the effect of these different treatments on 1PE-TRPL spectra data, which indicates reduced SRV in all cases. Cleaned samples resulted in surface recombination velocities approaching 1×10^5 cm/s. This improved SRVs by $\sim$2–3$\times$ after a removal of any detectable oxygen signature by XPS.

TABLE II. Summary of surface compositions extracted by XPS of various samples examined in this work.

	Atomic concentration (%)													
Sample treatment	Cd	Te	O	C	Br	Cu	Na	K	S	Cr	Fe	Si	Cl	Cd/Te
As-received	13.2	22.4	38.1	23.3								2.5	0.5	0.59
Br_2:MeOH	8.9	12.2	6.7	70.7	1.5									0.73
3 kV Ar^+	52.2	47.8												1.08
Atomic H	36.9	33.4	0.7	29.0										1.10
Ar^+, 250 °C UHV	52.1	47.9												1.09
Cd ampoule anneal	11.9	9.2	0.8	79.0										1.29
Te ampoule anneal	6.5	6.2	1.2	86.2										1.05
UV/O_3	25.5	14.0	51.4	9.1										1.81
$NaOH:Na_2S_2O_4$	39.5	29.3	5.1	9.4			2.3		14.5					1.35
KOH	23.9	21.4	11.2	42.5		0.9								1.12
Hydrazine	31.9	36.9	5.3	24.2										0.86
$CH_3COOH:HNO_3:H_2SO_4$	0.2	53.3	15.4	31.2										0.004
$FeCl_3$	0.8	23.5	43.9	28.3							3.5			0.03
$HNO_3:K_2Cr_2O_7:Cu(NO_3)_2$	3.0	35.5	46.8	11.1		3.1		0.5		5.3				0.08
$HNO_3:K_2Cr_2O_7$	0.9	14.5	19.5	17.0										0.06

UHV and ambient pressure thermal reconstructions

Several of the Br_2:MeOH/Ar sputter-cleaned single crystals (100) were annealed at 250 °C for 5 min in UHV to enable thermal reconstruction. Figure 4 and Table I show that surface reconstruction lowers the surface recombination velocity by an order of magnitude, to $\sim 3 \times 10^4$ cm/s. LEED indicates that this thermal reconstruction resulted in a $(2 \times 1)_{Cd}$ surface (Figure 4). There was no indication that longer annealing times yielded significant benefits or changes. The duration and ion-energy of the sputter-cleaning step is critical to remove the surface/sub-surface damage (e.g., a 5 min, 500 eV process was found to impart limited improvements, whereas 3 keV for 5 min was sufficient).

While the decreased SRV from the UHV sputter/anneal is encouraging, this type of UHV processing may be difficult to include in practical device processing. In an effort to develop a higher throughput passivation process that might replicate the UHV process, we studied a set of samples that were thermally annealed in an inert atmosphere with and without a wet chemical etch. One crystal was annealed as-received, one had a 2% Br_2:MeOH etch prior to annealing, and the last had a 2% Br_2:MeOH etch followed by a KOH etch prior to annealing. The Br_2:MeOH etch removed ca. 25 μm from the surface. While wet etches and their effect on stoichiometry will be discussed in further detail in the next section, the purpose of the KOH etch was to remove some of the Te and Te-oxides that might remain on the surface after the Br_2:MeOH etch. All three samples were then heated on a hotplate in a nitrogen-filled glovebox as described in the experimental section. 1PE-TRPL measurements were taken after each anneal step, and a peak near surface lifetime of 830 ps (SRV = 2.6×10^4 cm/s) was obtained from the sample that was etched in Br_2:MeOH/KOH and annealed (Figure 4). Comparing curves in Figure 4, or the parameters in Table I, we note that the optimized sputter-cleaning/vacuum anneal, Br_2:MeOH/hotplate anneal, and Br_2:MeOH/KOH/hotplate anneal treatments all result in very similar surface recombination velocities near 3×10^4 cm/s, even though they are arguably fairly different treatments. The sample that was only thermally annealed, without a chemical or ion-etch, showed some limited improvement compared to an as-received crystal. The increased SRV relative to the other methods is consistent with (sub)surface damage and/or contamination that is not remedied by a thermal surface reconstruction alone. These data suggest that some minimum level of etching is necessary to remove the surface damage prior to any thermal reconstruction, with the possibility that microns of material may need to be removed in polished samples.

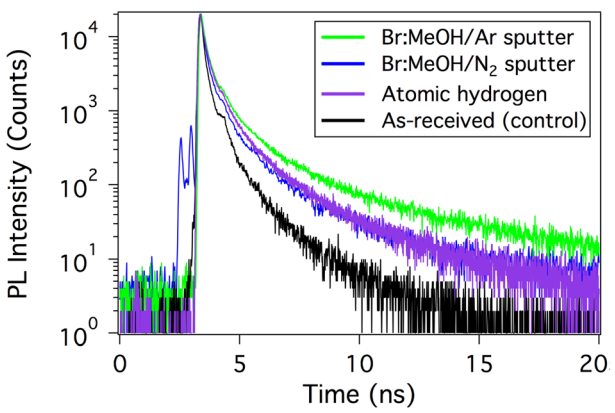

FIG. 3. 1PE-TRPL decays of single crystals treated with various stoichiometric UHV surface-cleaning methods.

Last, to confirm that this is indeed a surface passivation effect, we alternated surface treatments and were able to toggle surface recombination velocity between low and high values. This was achieved by performing a Br_2:MeOH etch followed by a short KOH etch (as above) prior to the hotplate anneal. After a minimum SRV was observed, the surface was reset by a Br_2:MeOH etch, thereby dramatically increasing the SRV, and the process was repeated to again reduce surface recombination. The second etch/anneal cycle has slightly improved surface recombination. This may be attributed to chemically removing more damaged subsurface material.

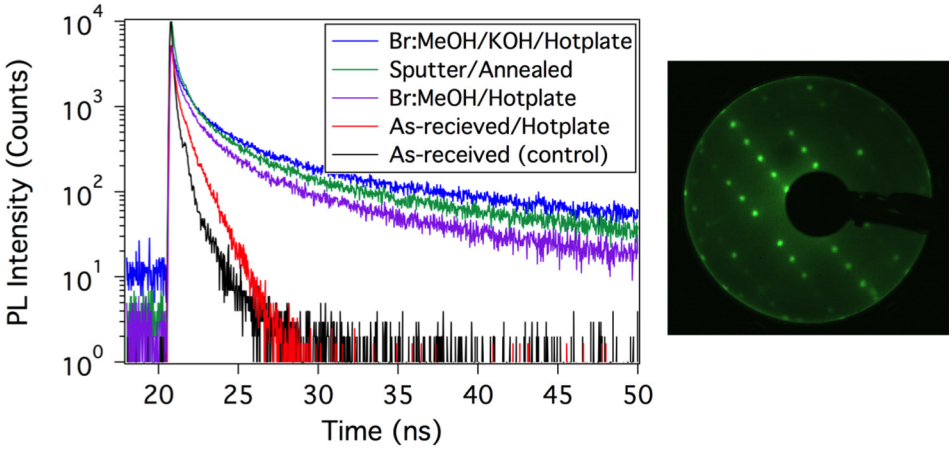

FIG. 4. (Left) 1PE-TRPL of thermally reconstructed single crystals. Curves include an as-received control and three samples annealed on a hotplate in a glovebox: an as-received crystal, a Br:MeOH etched crystal, and a Br:MeOH etched/KOH etched crystal. These can be compared to a crystal that was Br:MeOH etched, then sputter cleaned and thermally annealed in UHV. The three samples that had surface damage stripped with a Br:MeOH etch have similar TRPL decay curves. (Right) LEED pattern of a sputtered/annealed sample shows the $(2 \times 1)_{Cd}$ reconstructed surface.

The effects of varying stoichiometry on surface recombination subtractive (wet etches)

Cleaning and thermally reconstructing the surface resulted in a significant reduction of surface recombination, while maintaining a stoichiometric surface. We also tested the effect of shifting the surface stoichiometry on surface recombination. There are numerous wet etches/surface preparations that have been reported to alter the surface stoichiometry as measured by XPS or Auger Electron Spectroscopy (AES).[1,54,55] These stoichiometry shifts are sometimes small and hard to measure, which has led to some discrepancies between references, but there is general agreement that the stoichiometry is altered. We selected a variety of wet treatments that had been used historically with the CdTe system, including some of the most typical treatments seen as well as treatments that should result in either Te-rich or Cd-rich surfaces. We performed these etches on both as-received, single-crystals and as-deposited, large-grain polycrystalline films in both air and in a nitrogen-filled glovebox.

While stoichiometry variations in bulk CdTe without Te or Cd segregation are expected to be much less than the detection limits of XPS/AES (~0.1 at. % absolute differences), various treatments are known to shift the surface stoichiometry measurably by these techniques. However, there are inconsistencies between literature reports on the expected stoichiometry changes from each treatment in addition to large variations in reported treatment conditions. Hence, we used XPS to measure the surface stoichiometry after our specific treatments on single crystals. These measurements revealed a clear trend. Samples treated with oxidizers were left with strong elemental Te signatures and an overall Te-rich surface, with Br_2:MeOH being the closest to stoichiometric (0.73:1 Cd:Te). Samples treated with reducers were closer to stoichiometric, but with slightly Cd-rich surfaces. The KOH-treated sample had a 1.12:1 Cd:Te surface stoichiometry whereas the NaOH/$Na_2S_2O_4$-treated sample had a Cd:Te ratio of 1.35:1. The KOH-treated sample had small amounts Cu on the surface, as well as some oxygen and significant amounts of carbon. The NaOH/$Na_2S_2O_4$-treated sample was observed to have small amounts of Na and somewhat more S as well as C and O at the surface.

1PE-TRPL data for all samples showed that the shifts in surface stoichiometry correlated quite well with surface recombination velocity (Table I). Oxidized surfaces uniformly had high surface recombination velocities, with lifetimes near the limit of the instrument response. Reduced surfaces showed distinct improvements in lifetime and SRV (Figure 5, Table I). This trend was observed in single-crystal wafers and polycrystalline films, although the magnitude of the change was smaller in the single crystals. The smaller improvement observed in single crystals is likely due to polishing damage at the surface/subsurface of the single crystals that may remain even after a reducing etch.

Chemically removing the surface and subsurface damage from the single crystals before a reducing treatment should increase the magnitude of the improvement in the lifetime and SRV of the single crystals. We examined two different reducing treatments that followed a Br_2:MeOH etch to chemically remove damage. First, we used a Br_2:MeOH/N_2H_4 treatment. A similar treatment was used on n-type, In-doped ($1.5 \times 10^{16}\,cm^{-3}$) CdTe single crystals to achieve one of the lowest reported SRVs in the literature (200 cm/s).[2] In our p-type (100) CdTe crystals, this process shifted the surface stoichiometry from 0.73:1 Cd:Te (Br_2:MeOH only) to 0.86:1 Cd:Te. While the surface remained Te-rich, it was closer to stoichiometric after N_2H_4. There was also a modest improvement in the surface recombination velocity ($\sim 7 \times 10^4$ cm/s), but the resulting surface was not air stable with a relaxation back to the untreated state over the course of 1–2 h. This indicates that oxidation of a Te-rich surface increases surface recombination. Second, we examined the effect of a Br_2:MeOH etch followed by successive KOH etches with 1PE-TRPL measurements after each etch. While we found a similar reduction in surface recombination velocity (6.2×10^4 cm/s) compared to a KOH-only treatment ($6.6–9.1 \times 10^4$ cm/s), these treatments also could be overdone, such that the surface recombination would begin to increase again when over-etched with KOH. It is also worth noting that while the trend was repeated on multiple occasions with similar minima in SRV, the optimal etch time was not reproducible. We were able to establish that the kinetics were quite different depending on the KOH temperature (for instance, 15 s at 50 °C yielded similar SRV's to 300 s at 40 °C in one set of experiments), this was carefully controlled and not believed to be the primary source of error. Instead, we attribute the irreproducibility to a non-uniform

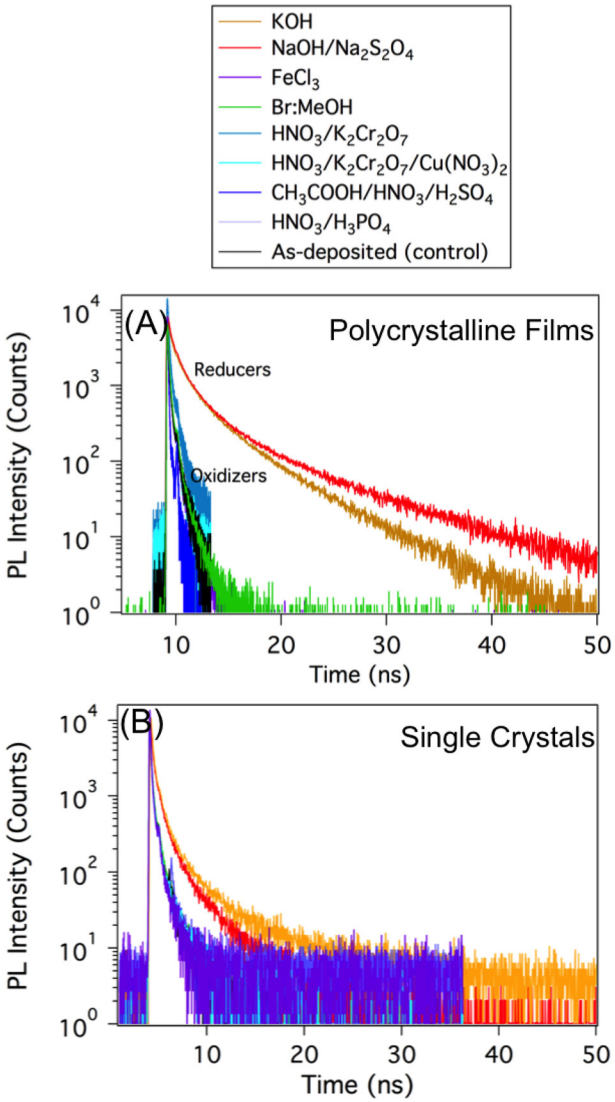

FIG. 5. 1PE-TRPL decay curves of (a) large grain polycrystalline films and (b) single crystals. Reducing treatments significantly diminished surface recombination, whereas oxidizing treatments yielded no improvement. The most aggressive oxidizing treatments (nitric/phosphoric acid and acetic/nitric/sulfuric acid) left samples with very low PL intensities, such that they were not measureable for the single crystal samples.

Br_2:MeOH etch rate and/or varying levels of subsurface damage/oxidation between crystals.

Additive (ampoule anneals and MBE growth)

To complete this study, we intentionally shifted the stoichiometry towards Te-rich and Cd-rich defect chemistries of single (100) crystals in the bulk and/or at the surface using additive methods—ampoule anneals and MBE depositions. Ampoule anneals in either a Cd- or Te-overpressure affect both the bulk and surface stoichiometry. Using available self-diffusion data,[56] estimates of the minimum characteristic diffusion length for Cd or Te in CdTe can each vary orders of magnitude ranging from microns to millimeters with our anneal conditions of 700 °C for 2 h in Cd- or Te-saturated conditions, respectively. We do not observe large variation over the crystal depth with 2PE-TRPL, indicating that the diffusion length is long (the crystals are 1 mm

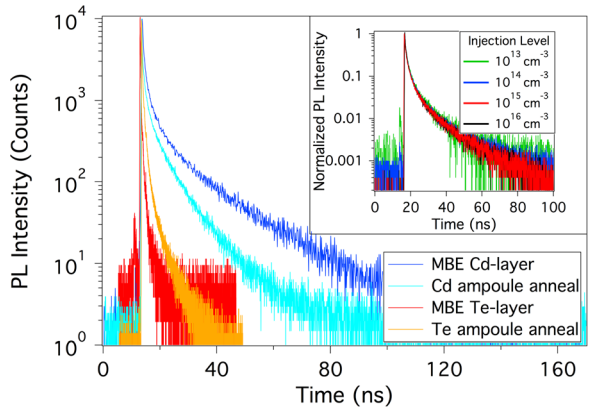

FIG. 6. 1PE-TRPL decays of single crystals with additive stoichiometry shifts as altered with ampoule annealing and MBE deposition. The ampoule anneals alter both the bulk and the surface, whereas the MBE should only alter the surface. (Inset) Surface recombination is invariant over the tested range of injection levels.

thick). In contrast, the short MBE step deposits a small amount of elemental Cd or Te on the sample surface without affecting the bulk. A summary of the samples' properties can be found in Table II, and a comparison of the 1PE-TRPL decays is shown in Figure 6.

Annealing a sample in a Te-overpressure increases doping levels (from low $10^{14}\,cm^{-3}$ to mid $10^{16}\,cm^{-3}$), but it decreases the bulk minority-carrier lifetime by more than an order of magnitude.[57] Furthermore, there is little to no improvement in passivation as measured SRV. Annealing in a Cd-overpressure converts the carrier type from p-type to n-type, but the carrier concentration remains in the mid-to-low $10^{14}\,cm^{-3}$ range.[44] τ_{bulk} (2PE-TRPL) remains ~100 ns and the surface recombination velocity decreases by an order of magnitude to $2–3 \times 10^4$ cm/s. XPS measurements of the surface reveal the Cd-rich anneal left a thin, <1 nm thick layer of elemental Cd layer on a surface that had an overall Cd:Te ratio of 1.28. The metallic nature of the cadmium over-layer was confirmed by ultraviolet photoemission spectroscopy (UPS) data showing a Fermi edge feature at 0 eV (Figure 7) and its thinness by virtue of the fact that the Fermi edge is not observed in the X-ray excited spectrum which

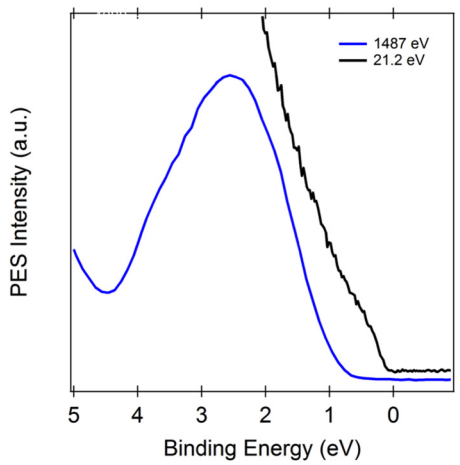

FIG. 7. X-ray and He I-excited valence band spectra of crystal after annealing in ampoule containing Cd^0.

has a larger effective probe depth (15–30 Å) than the UPS experiment (4–8 Å).[58]

MBE samples were used to provide clean control samples with abrupt Te or Cd layers grown on thermally reconstructed single-crystal surfaces. Cd layers were grown with nominal thicknesses from 2–11.7 nm. Te layers were grown with nominal thicknesses from 3.7–22.5 nm. The thickest layers investigated had poor photoluminescence, likely due to the poor penetration. The penetration depth for Cd at 650 nm, should be ~9.5 nm. For Te it should be ~25 nm.[48] As shown in Figure 6, a sample with an estimated 4.5 nm thick Cd layer had a near surface lifetime of 1.15 ns (SRV $\sim 1.9 \times 10^4$). In contrast, the best Te-capped samples yielded near surface lifetimes of ~40 to 100 ps. For the thinnest Te and Cd MBE grown layers (15 s flux compared to the optimal 35 s), there was no measureable difference with 1PE-TRPL ($\tau_1 \sim 95$ ps, SRV $\sim 2.3 \times 10^5$ cm/s). In fact, the unexposed backs of the samples were the same as the front suggesting no substantial deposition had occurred. These MBE growths perhaps provide the cleanest evidence that a Te-terminated surface is detrimental to surface recombination whereas a Cd-terminated surface provides a distinct benefit. They also provide a target thickness to realize these benefits.

Stability

We observed that Te-rich surfaces had poor SRVs or were unstable to air exposure. In the few instances where somewhat reduced SRVs were observed for samples with Te-rich surfaces (e.g., Br:MeOH/N_2H_4 treated), they would decay to the as-received values after minutes of exposure. Nominally stoichiometric and Cd-rich surfaces, however, exhibited impressive stability in air. Stoichiometric samples that were chemically etched, sputter cleaned, and thermally reconstructed were exposed to UV ozone, air exposure for weeks, and finally damp heat (45 °C/85% RH) for 9 h with no discernible change in SRV. The SRV of a Cd-annealed sample was unchanged after months of storage. The wet-etched samples with Cd-rich surfaces were stable over the course of hours to days.

Using high resolution XPS (Figure 8) on stoichiometric, Cd-rich, Te-rich, atmospheric pressure annealed, and oxidized stoichiometric crystals, we observed three Te oxidation states: Te^{2-}, Te^0, and Te^{4+}. We note that cadmium core levels show little dependence on chemical states, in contrast to tellurium. Te^{-2} (i.e., CdTe) is the only Te oxidation state present in unoxidized stoichiometric and Cd-rich samples. For unoxidized Te-rich samples, elemental (Te^0) tellurium is also present, as can be seen in Figure 8(b). Oxidation of a stoichiometric crystal causes the appearance of two additional chemical states, Te^{4+} ($3d_{5/2}$ at 575.84 eV), and a smaller amount of Te^0 at ~573 eV (Figure 8(a)). The Te^0 $3d_{5/2}$ peak position was found to vary somewhat depending on how the Te was produced (oxidative etching or evaporation), consistent with prior reports of elemental tellurium existing in variety of polymeric structures. The presence of Te^{4+} is most likely due to the formation of (benign) $CdTeO_3$. The small amount of elemental Te that appears

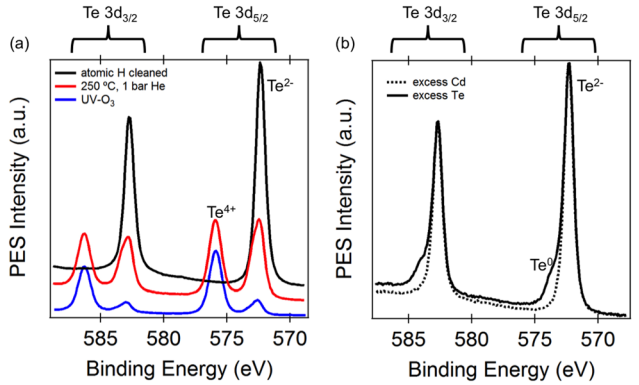

FIG. 8. High-resolution XPS spectra of the Te 3d region showing the three Te oxidation states observed in this work. We note that cadmium core levels show little dependence on chemical states, in contrast to tellurium. In the left panel, a CdTe(100) crystal cleaned by atomic hydrogen shows only the Te 3d spin-orbit doublet (Te $3d_{5/2}$: 572.29 eV. Oxidation of the crystal causes the appearance of two additional chemical states, Te^{4+} ($3d_{5/2}$ at 575.84 eV), and a smaller amount of Te^0 at ~573 eV. Panel (b) shows an example of Te^0 resulting from evaporation. Peak fitting was accomplished using PHI Multipak v9.5.1.0 using a Shirley background and the sum version of a Gaussian-Lorentzian function.

during the process of oxidizing the stoichiometric crystal does not increase surface recombination. We speculate that for oxidized Te-rich samples, in addition to this benign oxide that the continued overwhelming presence of Te^0 and/or formation of TeO_2 result in continued high surface recombination. For Cd-rich samples, this benign oxide or CdO may be formed. In this case, the presence of elemental Cd must overwhelm the effects of oxidation and/or the oxides must be benign.

Proposed mechanism for reduced surface recombination

The experiments outlined above illustrate that stoichiometric and Cd-rich surfaces exhibit reduced surface recombination after the removal of any damaged (sub)surface. This is in direct contrast to Te-rich surfaces, which have large SRVs.

Next, we discuss possible mechanisms for the observed effects. There are two general approaches to surface passivation. The first method is to confine the carriers, keeping them away from the surface. This can be achieved in multiple ways such as generating a potential barrier with a type one heterojunction or through strong doping of the surface region in such a way as to create electrostatic band bending to confine minority carriers to the bulk. We will call this "carrier confinement by potential barriers," or model 1. The second method is to reduce the density of recombination sites at the surface. This includes chemical passivation such as reducing the number of dangling/wrong bonds. One way to accomplish this is by cleaning and ordering a surface by sputter cleaning and annealing in UHV. We call this model 2—reduced interface density of states. It is possible that both mechanisms are present, but one is likely to be dominant.

Experimentally, these two limiting models of surface passivation can be distinguished by analyzing intensity dependence of the time-resolved spectroscopy data. In the

case of potential barriers (model 1), electric fields could be effectively screened if concentration of photogenerated carriers is sufficiently high. Our studies were limited to undoped CdTe with typical carrier concentration of $\sim 10^{14}$–$10^{15}\,cm^{-3}$. For such low doping, band bending at the surface could be effectively screened when the excitation power is in the range used in our studies.[59]

In the case of reduced density of states (model 2), a weaker surface recombination rate dependence on injection is expected. Figure 6 shows that when injection was changed from 10^{13} to $10^{16}\,cm^{-3}$ for a Cd-annealed sample, the near-surface recombination rate was approximately the same. Similar results were observed for other samples where variable injection studies were applied. Therefore, our data indicate that reduced SRV is largely due to decreased density of recombination centers near the CdTe surface.

In CdTe, the lowest energy surfaces are formed when the surface Te atoms dimerize to fill their dangling bonds and Cd atoms have empty dangling bonds.[60,61] We will now consider this in terms of the observed trends: Te-rich surfaces have high SRV, while Cd-rich surfaces have lower SRV.

The Te/CdTe band diagram has been experimentally measured and found to be thickness dependent.[40] For thin (<50 Å) Te, the Te has been measured to be n-type. Two bonding configurations, Cd—Te and Te—Te, are observed for thicknesses >1 Å, consistent with dimerization. The bandgap of Te is 0.33 eV, creating a Type I heterojunction, but in the wrong direction for carrier confinement (Figure 9(a)). The smaller bandgap coupled with its alignment causes both holes and electrons to accelerate towards the Te surface, rather than confining the carriers away from it. Furthermore, the dimerization of Te results in midgap states due to antibonding,[62,63] leading to a driving force of ~0.5 eV for both holes and electrons.

Cadmium is a metal, sometimes characterized as a transition or even a post-transition metal. In this work, we measured its Fermi energy to be offset relative to the valance band maximum of CdTe by 0.58 eV (Figure 9(b)). This indicates that in both Cd-rich and Te-rich surfaces, there is a significant potential gradient favoring both carrier types to move to the surface where the presence of defects can enable recombination. This suggests that the relative reduction in surface recombination observed for stoichiometric and Cd-rich surfaces is due to chemical passivation of these defects rather than carrier confinement.

When we examine the case of the oxidized stoichiometric crystal (Figure 8), we observed the formation of Te^0 in addition to Te^{4+}. These oxidized samples, however, maintained their reduced surface recombination. This suggests that either the quantity of Te^0 in these oxidized samples is lower or that the Te^0 does not dimerize to form the deleterious recombination states generated in Te-rich samples. This may be due to the way in which the benign $CdTeO_3$ interacts with the Te^0 and CdTe crystal.

CONCLUSION

As discussed in the introduction, solar cells based on polycrystalline CdTe can benefit from improved surface passivation and the concomitant reduction in surface recombination velocity. This becomes more important as bulk material properties improve and longer diffusion lengths allow carriers to reach these interfaces. We find that the near surface lifetimes/SRVs observed in untreated single crystals, large-grain polycrystalline films, and typical as-deposited polycrystalline films used in solar cells are comparable. Near surface lifetimes range from 4–90 ps ($2–50 \times 10^5$ cm/s), compared to bulk lifetimes of 6–14 ns for large grain polycrystalline films and 80–140 ns for single crystals. This suggests that surface recombination is a critical limitation in all of these materials.

We have examined several different passivation methods with both single crystals and large-grain polycrystalline films. Both of these materials have bulk lifetimes significantly longer than those observed in typical polycrystalline CdTe PV devices (1~3 ns). We have explored a variety of techniques (cleaning, thermal reconstruction, bulk defect chemistry shift, capping layers, and subtractive etches) to improve the lifetime without intentionally incorporating extrinsic dopants. We find that the best treatments in each category approach similar limiting values of near-surface minority-carrier lifetime/surface recombination velocity of ~800–1100 ps and $2–3 \times 10^4$ cm/s (Figure 10). This suggests that these approaches may be just different avenues to a similar end result, and that the processing window to achieve these improvements is fairly broad. They also suggest that

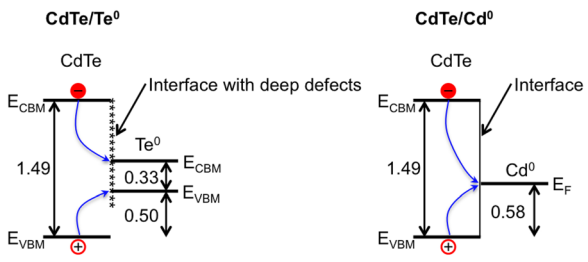

FIG. 9. Band alignment of CdTe with elemental tellurium (left panel) and of CdTe and elemental cadmium (right panel). Band energies in CdTe-Te case taken from Ref. 58, values in right figure for CdTe-Cd are our measurements. Both cases show a significant potential gradient favoring movement of both electrons and holes to the interface where the presence of defects can enable their recombination.

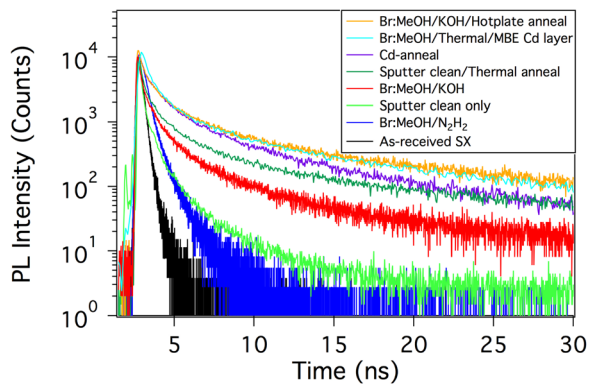

FIG. 10. Summary of some of the best treatments on single crystal CdTe samples. There is a progression of the effects of cleaning the sample, adjusting the surface stoichiometry, and ultimately reconstructing the surface.

there may be a limit to intrinsic passivation approaches. Reducing SRV much below 10^4 cm/s will likely require extrinsic passivants.

The lowest surface recombination resulted from a combination of steps. First, a cleaning/damage removal step may be necessary to remove surface contamination or subsurface damage. After this step, the surface was nearly stoichiometric or slightly Cd-rich. Last, a thermal reconstruction step restored surface crystallinity (in an inert atmosphere, UHV, or Cd-ambient) and significantly reduced SRV.

We believe the reduced surface recombination that we observed in stoichiometric and Cd-rich samples was due to chemical passivation that resulted in the elimination of many wrong and/or dangling bonds. Te-rich surfaces have a tendency to dimerize which introduce mid-gap states for additional recombination. In contrast, Cd-rich surfaces do not suffer from this. Furthermore, we observed that a reconstructed, stoichiometric surface maintained its reduced surface recombination even when exposed to heavy oxidization from UV ozone and damp heat. In the case of this heavy oxidation, XPS indicated the formation of $CdTeO_3$, which suggests it is a benign oxide.

Significant improvements in open-circuit voltage and efficiency require the ability to maintain high doping density and high minority carrier lifetimes both in the bulk and at the surface. We believe that back contact recombination is not the major limiting factor yet in CdTe PV, which is one of the reasons why Te-rich surface preparation has been used to make back contacts. However, as the bulk properties (i.e., doping and lifetime) improve, surface recombination will become one of the major bottlenecks to further advancement, just as was observed in Si and GaAs PV systems. Our work suggests that a Te-rich surface layer results in significant surface recombination. Furthermore, it suggests that a Cd-rich layer should lead to reduced surface recombination.

ACKNOWLEDGMENTS

The National Renewable Energy Lab was supported by the U.S. Department of Energy under Contract No. DE-AC36-08-GO28308. We acknowledge the support of the CdTe Solar program of the Solar Energy Technologies Office, Office of Energy Efficiency and Renewable Energy, U.S. Department of Energy. The U.S. Government retains and the publisher, by accepting the article for publication, acknowledges that the U.S. Government retains a nonexclusive, paid up, irrevocable, worldwide license to publish or reproduce the published form of this work, or allow others to do so, for U.S. Government purposes.

[1]J. P. Ponpon, "A review of ohmic and rectifying contacts on cadmium telluride," Solid-State Electron. **28**, 689–706 (1985).
[2]R. Cohen, V. Lyahovitskaya, E. Poles, A. Liu, and Y. Rosenwaks, "Unusually low surface recombination velocity and long bulk lifetime in n-CdTe single crystals," Appl. Phys. Lett. **73**, 1400–1402 (1998).
[3]W. K. Metzger, D. Albin, D. Levi, P. Sheldon, B. M. Keyes, and R. K. Arhenkiel, "Time-resolved photoluminescence studies of CdTe solar cells," J. Appl. Phys. **94**, 3549–3555 (2003).
[4]D. Kuciauskas, J. N. Duenow, A. Kanevce, J. V. Li, M. R. Young, P. Dippo, and D. Levi, "Optical-fiber-based, time-resolved photoluminescence spectrometer for thin-film absorber characterization and analysis of TRPL data for CdS/CdTe interface," in *Proceedings of 38th IEEE PVSC* (2011), pp. 001721–001726.
[5]L. Jastrzebski, J. Lagowski, and H. C. Gatos, "Application of scanning electronic microscopy to determination of surface recombination velocity: GaAs," Appl. Phys. Lett. **27**, 537–539 (1975).
[6]S. R. Lunt, G. N. Ryba, P. G. Santangelo, and N. S. Lewis, "Chemical Studies of the passivation of GaAs surface recombination using sulfides and thiols," J. Appl. Phys. **70**, 7449–7467 (1991).
[7]T. Lauinger, J. Schmidt, A. G. Aberle, and R. Hezel, "Record low surface recombination velocities on 1 Ω cm p-silicon using remote plasma silicon nitride passivation," Appl. Phys. Lett. **68**, 1232–1234 (1996).
[8]B. Hoex, S. B. S. Heil, E. Langereis, M. C. M. van de Sanden, and W. M. M. Kessel, "Ultralow surface recombination of c-Si substrates passivated by plasma-assisted atomic layer deposited Al_2O_3," Appl. Phys. Lett. **89**, 042112 (2006).
[9]E. Yablonovitch, D. L. Allara, C. C. Chang, T. Gmitter, and T. B. Bright, "Unusually low surface-recombination velocity on silicon and germanium surfaces," Phys. Rev. Lett. **57**, 249–252 (1986).
[10]A. G. Aberle, "Surface passivation of crystalline Si solar cells: A review," Prog. Photovolt.: Res. Appl. **8**, 473–487 (2000).
[11]J. M. Olson, R. K. Ahrenkiel, D. J. Dunlavy, B. Keyes, and A. E. Kibbler, "Ultralow recombination velocity at $Ga_{0.5}In_{0.5}P$/GaAs heterointerfaces," Appl. Phys. Lett. **55**, 1208–1210 (1989).
[12]J. M. Olson, S. R. Kurtz, A. E. Kibbler *et al.*, "In recent advances in high efficiency GaInP2/GaAs tandem solar cells," in *Proceedings of IEEE 21st PVSC, Kissismee, FL* (1990), pp. 24–20.
[13]See http://www.firstsolar.com for information on the leading CdTe company in the world, which at the time of publishing this article had the lowest unsubsidized production cost per watt of any PV technology in the world and was producing >2 GW/yr (accessed June 14, 2014).
[14]See http://www.greentechmedia.com/articles/read/the-global-pv-manufacturing-landscape-in-2012-and-beyond-a-brave-new-world for Fig. 6 which illustrates the point (accessed June 26, 2014).
[15]M. A. Green, K. Emery, D. L. King, S. Igari, and W. Warta, "Solar cell efficiency tables (version 19)," Prog. Photovolt.: Res. Appl. **10**, 55–61 (2002).
[16]M. A. Green, K. Emery, Y. Hishikawa, W. Warta, and E. D. Dunlop, "Solar cell efficiency tables (version 39)," Prog. Photovolt.: Res. Appl. **20**, 12–20 (2012).
[17]M. A. Green, K. Emery, Y. Hishikawa, W. Warta, and E. D. Dunlop, "Solar cell efficiency tables (version 40)," Prog. Photovolt.: Res. Appl. **20**, 606–614 (2012).
[18]M. A. Green, K. Emery, Y. Hishikawa, W. Warta, and E. D. Dunlop, "Solar cell efficiency tables (version 41)," Prog. Photovolt.: Res. Appl. **21**, 1–11 (2013).
[19]M. A. Green, K. Emery, Y. Hishikawa, W. Warta, and E. D. Dunlop, "Solar cell efficiency tables (version 42)," Prog. Photovolt.: Res. Appl. **21**, 827–837 (2013).
[20]M. A. Green, K. Emery, Y. Hishikawa, W. Warta, and E. D. Dunlop, "Solar cell efficiency tables (version 45)," Prog. Photovolt.: Res. Appl. **23**, 1–9 (2015).
[21]A. Kanevce and T. A. Gessert, "Optimizing CdTe solar cell performance: impact of variations in minority–carrier lifetime and carrier density profile," IEEE J. Photovolt. **1**, 99–103 (2011).
[22]J. Sites and J. Pan, "Strategies to increase CdTe solar-cell voltage," Thin Sol. Films **515**, 6099–6102 (2007).
[23]J. N. Duenow, J. M. Burst, D. S. Albin, D. Kuciauskas, S. W. Johnston, R. C. Reedy, and W. K. Metzger, "Single-crystal CdTe solar cells with Voc greater than 900 mV," Appl. Phys. Lett. **105**, 053903 (2014).
[24]V. Lyahovitskaya, L. Chernyak, J. Greenberg, L. Kaplan, and D. Cahen, "Low temperature, postgrowth self-doping of CdTe single crystals due to controlled deviation from stoichiometry," J. Appl. Phys. **88**, 3976–3981 (2000).
[25]T. A. Gessert, S.-H. Wei, J. Ma, D. S. Albin, R. G. Dhere, J. N. Duenow, D. Kuciauskas, A. Kanevce, T. M. Barnes, J. M. Burst, W. L. Rance, M. O. Reese, and H. R. Moutinho, "Research strategies toward improving thin-film CdTe photovoltaic devices beyond 20% conversion efficiency," Sol. Energy Mater. Sol. Cells **119**, 149–155 (2013).
[26]J. D. Major, Y. Y. Proskuryakov, and K. Durose, "Impact of cadmium-rich back surfaces on cadmium chloride treatment and device performance in close space sublimation deposited CdTe solar cells," in *Proceedings of IEEE 37th PVSC* (2011), pp. 3537–3541.

[27]Y. Y. Proskuryakov, K. Durose, B. M. Taele, G. P. Welch, and S. Oelting, "Admittance spectroscopy of CdTe/CdS solar cells subjected to varied nitric-phosphoric etching conditions," J. Appl. Phys. **101**, 014505 (2007).
[28]C. S. Ferekides, D. Marinskiy, V. Viswanathan, B. Tetali, V. Palekis, P. Selvaraj, and D. L. Morel, "High efficiency CSS CdTe solar cells," Thin Solid Films **361**, 520–526 (2000).
[29]D. Bonnet, "Manufacturing of CSS CdTe solar cells," Thin Solid Films **361**, 547–552 (2000).
[30]D. L. Bätzner, A. Romeo, H. Zogg, R. Wendt, and A. N. Tiwari, "Development of efficient and stable back contacts on CdTe/CdS solar cells," Thin Solid Films **387**, 151–154 (2001).
[31]S. S. Hegedus and B. E. McCandless, "CdTe contacts for CdTe/CdS solar cells: effect of Cu thickness, surface preparation and recontacting on device performance and stability," Sol. Energy Mater. Sol. Cells **88**, 75–95 (2005).
[32]A. J. Nelson and D. Levi, "Novel method for growing CdS on CdTe surfaces for passivation of surface states and heterojunction formation," J. Vac. Sci. Technol. A **15**, 1119–1123 (1997).
[33]Yu. V. Klevkov, S. A. Kolosov, and A. F. Plotnikov, "Effect of passivation of the p-CdTe surface in $(NH_4)_sS_x$ on the current-voltage characteristics of contacts," Semiconductors **40**, 1048–1051 (2006).
[34]Y.-H. Kim, S.-Y. An, J.-Y. Lee, I. Kim, and K.-N. Oh, "Photoluminescence study on the effects of the surface of CdTe by surface passivation," J. Appl. Phys. **85**, 7370–7373 (1999).
[35]T. L. Chu, S. S. Chu, and S. T. Ang, "Surface passivation and oxidation of cadmium telluride and properties of metal oxide CdTe structures," J. Appl. Phys. **58**, 3206–3210 (1985).
[36]J. Ma, D. Kuciauskas, D. Albin, R. Bhattacharya, M. Reese, T. Barnes, J. V. Li, T. Gessert, and S-H. Wei, "Dependence of the minority-carrier lifetime on the stoichiometry of CdTe using time-resolved photoluminescence and first-principles calculations," Phys. Rev. Lett. **111**, 067402–067406 (2013).
[37]S.-H. Wei and S. B. Zhang, Phys. Rev. B **66**, 155211 (2002).
[38]T. A. Gessert, J. M. Burst, S.-H. Wei, J. Ma, D. Kuciauskas, W. L. Rance, T. M. Barnes, J. N. Duenow, M. O. Reese, J. V. Li, M. R. Young, and P. Dippo, "Pathways toward higher performance CdS/CdTe devices: Te exposure of CdTe surface before ZnTe:Cu/Ti contacting," Thin Solid Films **535**, 237–240 (2013).
[39]G. Teeter, "X-ray and ultraviolet photoemission spectroscopy measurements of Cu-doped CdTe (111)-B: Observation of temperature-reversible Cu_xTe precipitation and effect on ionization potential," J. Appl. Phys. **102**, 034504 (2007).
[40]D. W. Niles, X. Li, P. Sheldon, and H. Höchst, "A photoemission determination of the band diagram of the Te/CdTe interface," J. Appl. Phys. **77**, 4489–4493 (1995).
[41]Y. Nemirovsky and G. Bahir, "Passivation of mercury cadmium telluride surfaces," J. Vac. Sci. Technol. A **7**, 450–459 (1989).
[42]E. Finkman and S. E. Schacham, "Surface recombination velocity studies of anodic sulfide and ZnS coated HgCdTe," J. Vac. Sci. Technol. A **7**, 464–468 (1989).
[43]C. K. Kang, Sh. U. Yuldashev, J. H. Leem, Y. S. Ryu, J. K. Hyun, H. S. Jung, H. J. Kim, T. W. Kang, H. I. Lee, Y. D. Woo, and T. W. Kim, "Surface passivation by sulfur treatment of undoped p-type CdTe (100)," J. Appl. Phys. **88**, 2013–2015 (2000).
[44]M. O. Reese, J. M. Burst, C. L. Perkins, A. Kanevce, S. W. Johnston, D. Kuciauskas, T. M. Barnes, and W. K. Metzger, "Surface passivation of CdTe Single Crystals," IEEE J. Photovolt. **5**, 382–385 (2015).
[45]H. Wang, K. S. Wong, B. A. Foreman, Z. Y. Yang, and G. K. L. Wong, "One- and two-photon-excited-time-resolved photoluminescence investigations of bulk and surface recombination dynamics in ZnSe," J. Appl. Phys. **83**, 4773–4776 (1998).
[46]D. Kuciauskas, A. Kanevce, J. M. Burst, J. N. Duenow, R. Dhere, D. S. Albin, D. H. Levi, and R. K. Ahrenkiel, "Minority carrier lifetime analysis in the bulk of thin-film absorbers using subbandgap (two-photon) excitation," IEEE J. Photovolt. **3**, 1319–1324 (2013).
[47]E. S. Bernard, E. T. Hoke, S. T. Connor, J. R. Groves, T. Kuykendall, Z. Yan, E. C. Samulon, E. D. Bourret-Courchesne, S. Aloni, P. J. Schuck, C. H. Peters, and B. E. Hardin, "Probing carrier lifetimes in photovoltaic materials using subsurface two-photon microscopy," Sci. Rep. **3**, 2098–2106 (2013).
[48]E. D. Palik and G. Ghosh, *Handbook of Optical Constants of Solids* (Elsevier Science Publishing Co Inc, 1998).
[49]R. K. Ahrenkiel and J. Dashdorj, "Interface recombination velocity measurements by a contactless microwave technique," J. Vac. Sci. Technol. B **22**, 2063–2067 (2004).
[50]C. L. Perkins and L. S. Hasoon, "Surfactant-assisted growth of CdS thin films for photovoltaic applications," J. Vac. Sci. Technol. A **24**, 497–504 (2006).
[51]B. Stafford, Private communication, University of Illinois, Chicago (2015).
[52]J. F. S. W. F. Moulder, P. E. Sobol, and K. D. Bomben, *Handbook of X-ray Photoelectron Spectroscopy* (Perkin-Elmer Corporation, Eden Prairie, 1992).
[53]L. S. Hirsch, Z. Yu, S. L. Buczkowski, T. H. Myers, and M. R. Richards-Babb, "The use of atomic hydrogen for substrate cleaning for subsequent growth of II-VI semiconductors," J. Electron. Mater. **26**, 534–541 (1997).
[54]A. J. Ricco, H. S. White, and M. S. Wrighton, "X-ray photoelectron and Auger electron spectroscopic study of the CdTe surface resulting from various surface pretreatments: Correlation of photoelectrochemical and capacitance potential behavior with surface chemical composition," J. Vac. Sci. Technol. A **2**, 910–915 (1984).
[55]W. J. Danaher, L. E. Lyons, M. Marychurch, and G. C. Morris, "Chemical etching of crystal and thin film cadmium telluride," Appl. Surf. Sci. **27**, 338–354 (1986).
[56]L. Shcherbak, O. Kopach, P. Fochuk, A. E. Bolotnikov, and R. B. James, "Empirical correlations between the Arrhenius' parameters of impurities' diffusion coefficients in CdTe crystals," J. Phase Equilib. Diff. **36**, 99–109 (2015).
[57]J. M. Burst, M. O. Reese, D. S. Albin, S. B. Farrell, J. N. Duenow, T. Ablekim, S. K. Swain, K. G. Lynn, D. Kuciauskas, and W. K. Metzger, "Resetting the defect chemistry in CdTe to overcome longstanding stability and photovoltage limits," (unpublished).
[58]J. C. Green, "Photoelectron spectroscopy study of valence bands in solids," Ann. Rev. Phys. Chem. **28**, 161–183 (1977).
[59]D. Kuciauskas, A. Kanevce, P. Dippo, S. Seyedmohammadi, and R. Malik, "Minority-carrier lifetime and surface recombination velocity in single-crystal CdTe," IEEE J. Photovolt. **5**, 366–371 (2015).
[60]W. Mönch, *Semiconductor Surfaces and Interfaces*, 3rd ed. (Springer, 2001), p. 162.
[61]M. Ahr and M. Biehl, "Flat (0 0 1) surfaces of II-VI semiconductors: a lattice gas model," Surf. Sci. **505**, 124–136 (2002).
[62]I. M. Dharmadasa, "Recent developments and progress on electrical contacts to CdTe, CdS, and ZnSe with special reference to barrier contacts to CdTe," Prog. Cryst. Growth Charact. **36**, 249–290 (1998).
[63]S. C. Boehme, J. M. Azpiroz, Y. Aulin, F. C. Grozema, D. Vanmaekelbergh, L. D. A. Siebbles, I. Infante, and A. J. Houtepen, "Density of trap states and Auger-mediated electron trapping in CdTe quantum-dot solids," Nano. Lett. **15**, 3056 (2015).